

KARVE: A NANOPARTICLE ACCELERATOR FOR SPACE THRUSTER APPLICATIONS*

J. W. Lewellen[†], L. Danielson, A. Essunfeld, J. Hollingsworth, M.A. Holloway
Los Alamos National Laboratory, Los Alamos, NM, USA
E. Lewis, NASA Johnson Space Center, Houston, TX, USA

Abstract

We present a concept for using radiofrequency (RF)-based acceleration of nanoparticles (NPs) as a means of generating thrust for future space missions: the Kinetic Acceleration & Resource Vector Engine (KARVE) thruster. Acceleration of NPs via DC accelerators has been shown to be feasible in dust accelerator labs such as the Heidelberg dust accelerator [1] and the 3-MV hypervelocity dust accelerator at the Colorado Center for Lunar Dust and Atmospheric Studies [2]. In contrast, KARVE uses RF-driven acceleration of NPs as the basis of a thruster design lying between chemical and ion engines in performance: more efficient than chemical engines in terms of specific impulse; and higher thrust than ion engines. The properties of multi-gap RF accelerators also allow an on-the-fly tradeoff between specific impulse and thrust.

In this paper, we focus on the specifics of the KARVE thruster as an accelerator.

INTRODUCTION

Spacecraft typically rely on one of several types of thrust-generating engines for propulsion. The classic chemical-fuel rockets, such as those used to lift payloads to earth orbit and beyond, can provide high thrust, but are typically inefficient in terms of thrust delivered per unit mass of propellant consumed. Nuclear thermal propulsion (NTP) engines rely on a nuclear reactor, rather than the combustion process, to heat an exhaust gas, but can otherwise be thought of as similar to chemical rockets. Ion engines, essentially small DC guns accelerating ionized gas, provide high efficiency but low levels of thrust. Also, except in very rare (and presently unrealized) circumstances, spacecraft cannot refuel mid-flight, especially if traveling beyond earth orbit.

One result of the limitations of this tradespace is that, to date, there is no explicit viable design for a deep-space transport (DST) for crewed missions beyond the Moon that would reduce the nominal Mars mission orbital time substantially below 1,100 days [3, 4]. Studies considered conventional chemical propulsion, NTP, and ion/solar electric propulsion (SEP) for DST; but chemical rockets require too much fuel mass, NTP is too costly to develop, and SEP is too slow to guarantee mission success [3, 4]. Utilizing abundant lunar-regolith-derived NPs as fuel, we estimate a continuous-thrust theoretical limit travel time from the Moon to Mars of approximately 70 days.

We propose to adapt particle accelerator technology to accelerate NPs as a means of generating thrust. Initial calculations show that NPs can also be accelerated using radio-frequency (RF) based accelerators. As is the case with terrestrial electron, proton, and ion accelerators, RF-based acceleration removes the requirement for large DC stand-offs for obtaining high particle energies. We expect to achieve thrust capabilities on the order of 1 - 2 N/kW of power provided. In addition, we can utilize conventional beam optics techniques to add wide-angle thrust vectoring, a unique feature of KARVE compared to other engine concepts.

Finally, we anticipate that, with few possible exceptions, the performance of a KARVE engine will be insensitive to the exact composition of the NPs used as fuel. This allows for the possibility of in-flight refueling, by generating nanoparticles from local materials (e.g. lunar regolith, a nearby asteroid, etc.) via any of several techniques.

ACCELERATOR CONCEPT

Basic Design Considerations

In general, the higher the charge-to-mass ratio (q/m) of a particle, the easier it is to accelerate to relativistic velocities. Nanoparticles will have q/m ratios significantly lower than heavy ions, yet, are still amenable to RF-based acceleration schemes with appropriate selection of RF frequency and gap voltage.

In an RF accelerator, ideally a particle transits an accelerating gap in half of an RF period, so the length of the accelerating gap is half of the free-space wavelength, multiplied by the particle's normalized velocity:

$$L_g = \frac{1}{2} \beta \lambda_{rf} = \frac{\beta c}{2f_{rf}}, \quad (1)$$

where L_g is the gap length, βc is the particle velocity, and λ_{rf} and f_{rf} are the RF wavelength and frequency, respectively.

A 6-nm diameter iron NP will contain approximately 9600 iron atoms and have a mass of approximately $5.3 \cdot 10^5$ atomic mass units (AMU), or $5 \cdot 10^8$ MeV/c². We presume we can remove (or add) 10 electrons to the nanoparticle, for a net charge on a nanoparticle of $1.602 \cdot 10^{-18}$ C; the sign of the charge is irrelevant to the following estimates.

For initial acceleration, we posit a small, 20-kV DC pre-accelerator; given the above parameters for mass and charge, nanoparticles will exit the pre-accelerator at a speed of ~ 8.5 km/s, or $2.8 \cdot 10^{-5}$ c. If we posit a nominal accelerating gap length of 1 cm, then Eq. (1) suggests an RF frequency of 0.42 MHz.

While significantly below the operating frequencies of

* Work supported in part by the Los Alamos LDRD program.

[†] jwlewellen@lanl.gov

Content from this work may be used under the terms of the CC BY 3.0 licence (© 2021). Any distribution of this work must maintain attribution to the author(s), title of the work, publisher, and DOI

most modern accelerators, this frequency is well-suited to a Widerøe-like accelerator (RF-driven, but no resonant cavities) [5-7]. Reasonably powerful and efficient RF sources are available in this frequency range.

Initial Simulations

We performed a preliminary simulation of a model, 1-stage nanoparticle accelerator using General Particle Tracer (GPT) [8]. The model system presumes an incoming, gated stream of nanoparticles, mass and charge as described above, at 20 kV. This is followed by a short-gap buncher, a bunching drift, and then an accelerating gap; both the bunching and accelerating gaps are assumed to be parallel plates with uniform field between the plates.

Figure 1 shows the conceptual layout of the accelerator. Figure 2 shows the longitudinal phase-space evolution of the beam as it passes along the model system, along with a series of “snapshots” of the beam as it progresses along the

model accelerator. In the model, both the buncher and accelerator gap are 1 cm long; the peak electric field in the accelerating gap is 2 MV/m.

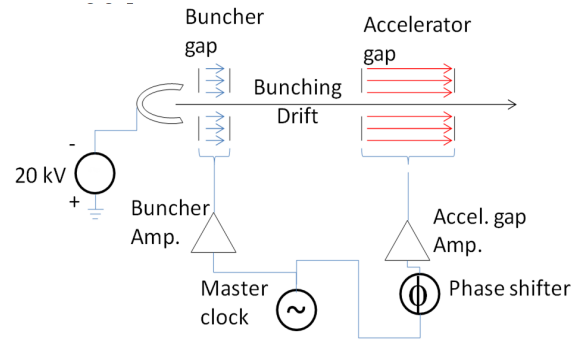


Figure 1: Conceptual layout of a model single-stage nanoparticle accelerator.

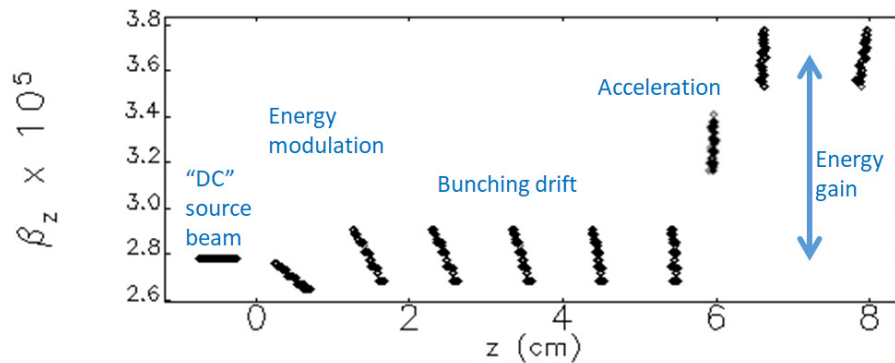


Figure 2: Evolution of the longitudinal phase-space of the beam as it progresses along the model accelerator.

For the model, the beam emission was gated to 1/2 of an RF period, or 1.2 μs. The average beam voltage increased to approximately 34 kV. This is in accord with the expected energy gain, taking the gap transit-time factor into account.

We note that the general evolution of the beam through the model accelerator is analogous to that of other RF accelerators with DC beam sources.

PERFORMANCE FIGURES

Thrust, Specific Impulse, and Power Use

The specific impulse, I_{sp} , provides a measure of how efficiently a thruster uses its fuel [Eq. (2)]. Specific impulse is defined as

$$I_{sp} = v_e/g, \quad (2)$$

where v_e is the velocity of the exhaust, and g is the acceleration due to gravity at the surface of the earth, 9.8 m/s². The units of I_{sp} are therefore seconds. I_{sp} provides a measure of the performance available from a particular type of fuel, without stating anything about the absolute thrust levels to be generated; all else equal, a fuel with a higher I_{sp} can provide a higher total impulse, and therefore velocity change, per unit mass of propellant consumed.

The thrust generated by an engine is given by

$$F_{th} = v_e \frac{dm}{dt} = I_{sp} g \frac{dm}{dt}, \quad (3)$$

where F_{th} is the thrust produced and dm/dt is the mass flow rate of the propellant.

In the case of the KARVE engine concept, as in an ion thruster, the thrust developed can be related to the average beam current and voltage, and thus, to the power required to accelerate the beam.

Presuming the nanoparticle beam remains in the nonrelativistic regime, I_{sp} for a KARVE engine in terms of the accelerator operating parameters can be calculated via

$$I_{sp} = \sqrt{\frac{2 N_g V_g Q_{np}}{m_{np} g^2}}, \quad (4)$$

where V_g is the voltage gain of the beam through a single accelerating gap, Q_{nm} is the total charge per nanoparticle, and m_{np} is the nanoparticle mass. N_g is the number of accelerating gaps in the KARVE thruster, with a presumption that each gap provides the same net voltage gain. The mass flow rate for the nanoparticle beam is

$$\frac{dm}{dt} = m_{np} I / Q_{np}, \quad (5)$$

where m_{np} and Q_{nm} are the nanoparticle mass and charge, respectively, and I is the average beam current. Finally, combining Eqs. (3), (4) and (5), the thrust from a KARVE engine, F_K , is given by

$$F_K = I \sqrt{\frac{2N_g V_g m_{np}}{Q_{np}}} \quad (6)$$

A 1-A beam at 100 kV, for the nanoparticle mass and charge given above, provides a thrust of approximately 10.5 N, with a specific impulse of $1.9 \cdot 10^3$ s. The beam power is 100 kW.

As KARVE is an RF-based accelerator; making the approximations that the RF power system is 50% efficient, and essentially all of the RF power is transferred to the beam (i.e., heavily beam-loaded), roughly 52 mN thrust per kW of “bus” power is generated.

For comparison, the specific impulse of liquid oxygen-liquid hydrogen fuel is 450 s. The I_{sp} of the NSTAR electrostatic xenon ion thruster ranges from 1950 s to 3100 s, and has a thrust-to-power ratio of 44 mN/kW.

Basic Design Considerations

A KARVE thruster with multiple accelerating gaps provides a unique ability to dynamically tailor its performance by varying its specific impulse. Specifically, it can switch from a higher-efficiency, lower-thrust mode, to a lower-efficiency but higher-thrust mode, without requiring any physical reconfiguration.

The RF system may be arranged such that the RF power, instead of being divided equally among all accelerating gaps, can instead be shunted to a subset of the total number of gaps in the KARVE thruster. The point of doing this, combined with the ability to vary the beam current from the nanoparticle source, is to allow the KARVE thruster to access different performance regimes, for a fixed power budget.

Consider a 5-gap KARVE engine, with a nominal voltage gain of 20 kV per gap. With all gaps powered and a 1-A beam, the KARVE engine would provide thrust of 10.5 N as described above. However, via reconfiguring the RF system, a 5-A beam could be accelerated through a single 20-kV gap for the same total beam power. In this case, according to Eq. (6), the thrust would increase by a factor of $\sqrt{5}$, to 23.4 N, or 117 mN/kW, for the same power consumption (the specific impulse would experience a corresponding drop by the same factor.). Figures 3 and 4 show I_{sp} and thrust per unit beam power, respectively, for several beam voltages and charges per nanoparticles. Both figures assume 6-nm diameter iron nanoparticles.

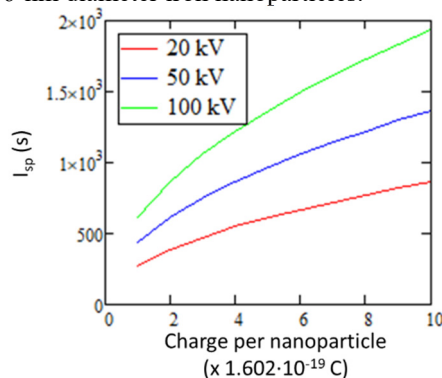


Figure 3: I_{sp} as a function of beam voltage and charge per nanoparticle.

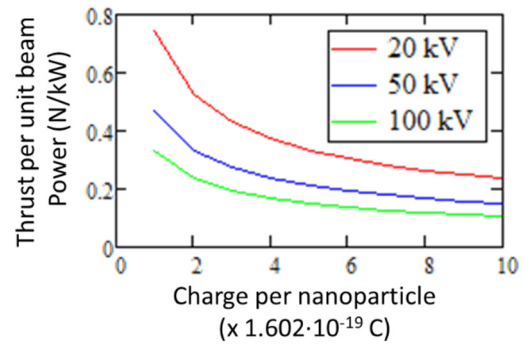


Figure 4: Thrust per unit beam power, versus beam voltage and charge per nanoparticle. (this does not include RF power system efficiency).

CONCLUSIONS

We have performed initial scoping studies for the performance of a nanoparticle accelerator, KARVE, intended to be used as a thruster for space applications. Its performance fills the gap between conventional rocket fuels and ion engines. RF acceleration allows access to high beam voltages, and the basic design concept allows access to a broad tradespace between efficiency and thrust, for a given power load on the spacecraft.

REFERENCES

- [1] A. Mocker *et al.*, “A 2 MV Van de Graaff accelerator as a tool for planetary and impact physics research”, *Rev. Sci. Instrum.*, vol. 82, p. 095111, Sep. 2011. doi:10.1063/1.3637461
- [2] A. Shu *et al.*, “3 MV hypervelocity dust accelerator at the Colorado Center for Lunar Dust and Atmospheric Studies”, *Rev. Sci. Instrum.*, Vol. 83, p. 075108, Jul. 2012. doi:10.1063/1.4732820
- [3] E. Linck *et al.*, “Evaluation of a Human Mission to Mars by 2033”, IDA Science and Technology Policy Institute, D-10510, Virginia, USA, Feb. 2019.
- [4] T. Cichan *et al.*, “Mars Base Camp: An Architecture for Sending Humans to Mars”, *New Space*, vol. 5, no. 4, pp. 203-218, Dec. 2019. doi:10.1089/space.2017.0037
- [5] R. Widerøe, “Über ein neues Prinzip zur Herstellung hoher Spannungen”, *Archiv für Elektrotechnik*, vol. 21, no. 4, pp. 387-406, Jul. 1928.
- [6] S. Humphries Jr., “Radio-frequency linear accelerators”, *Principles of Charged Particle Acceleration*, Mineola, NY, USA: Dover, pp. 452-459, 2012.
- [7] T. Wangler, “Standard linac structures”, *Principles of RF Linear Accelerators*, New York, NY, USA: Wiley, pp. 93-95, 1998.
- [8] Pulsar Physics, www.pulsar.nl